Supporting Information

Sub-Parts-per-Trillion Level Detection of Analytes by Superhydrophobic Preconcentration Paper Spray Ionization Mass Spectrometry (SHPPSI MS)

Pallab Basuri, Avijit Baidya, and Thalappil Pradeep*

DST Unit of Nanoscience (DST UNS) and Thematic Unit of Excellence,
Department of Chemistry, Indian Institute of Technology Madras,
Chennai 600036, India.
*E-mail: pradeep@iitm.ac.in,
Fax: 91-44-2257 0545

Table of contents

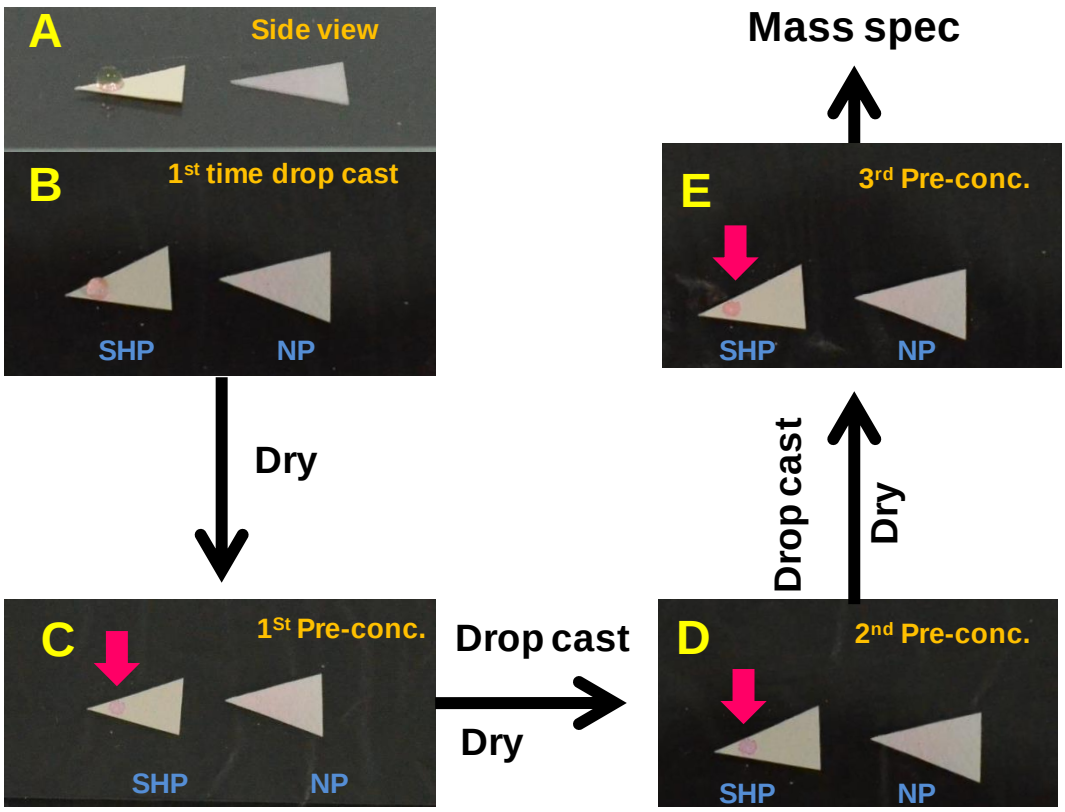

Figure S1. Optical images of the pre-concentration steps involved in SHPPSI MS using normal paper and superhydrophobic paper.

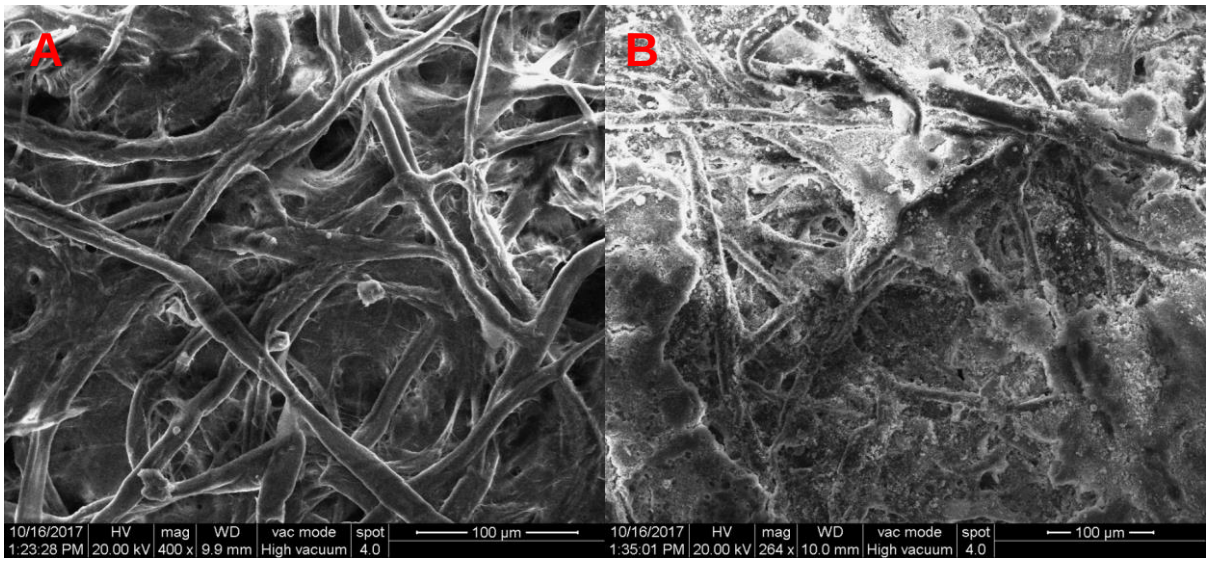

Figure S2. Comparative SEM images of a A) normal paper and B) superhydrophobic paper at different magnifications.

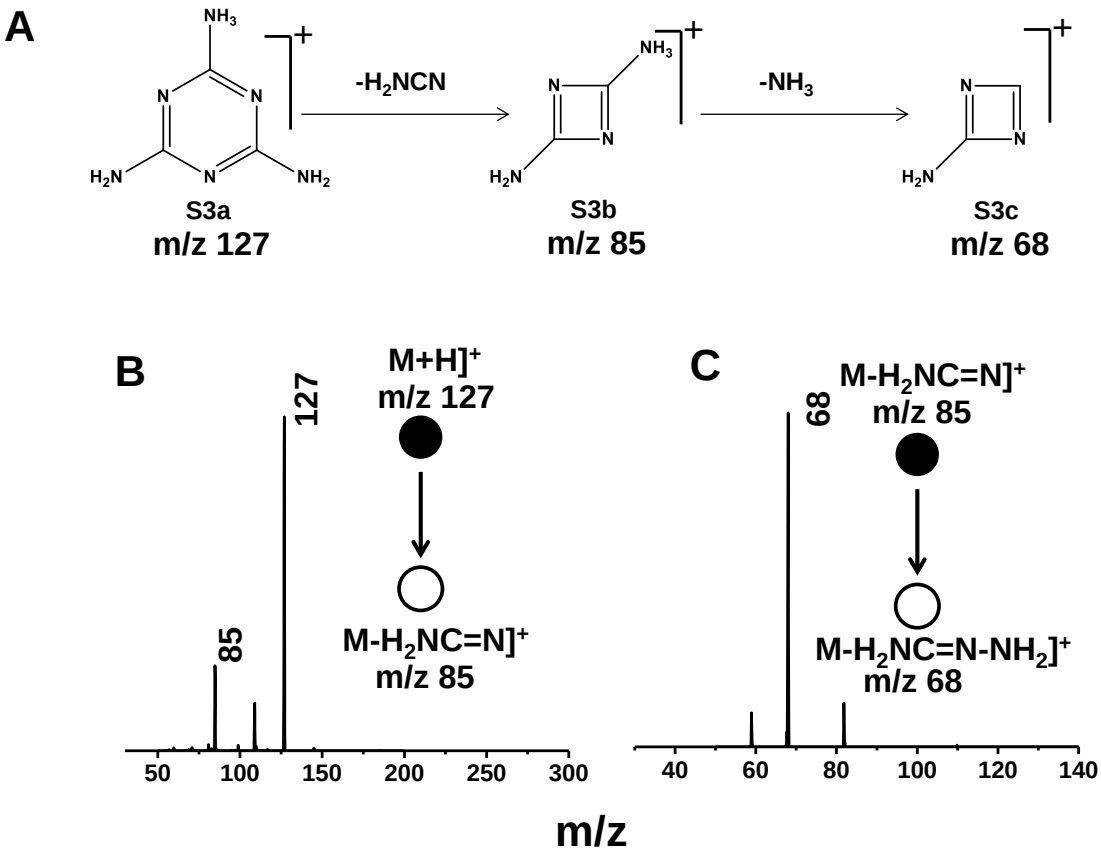

Figure S3. MS^2 and MS^3 spectra of melamine at 1.2 ppt (10 pM) in solution. A) Structures of the fragments; B) and C) are the MS^2 and MS^3 spectra of peaks at m/z 127 and 85. The fragmentation patterns and the structures of the fragmented ions were confirmed from the literature.[1]

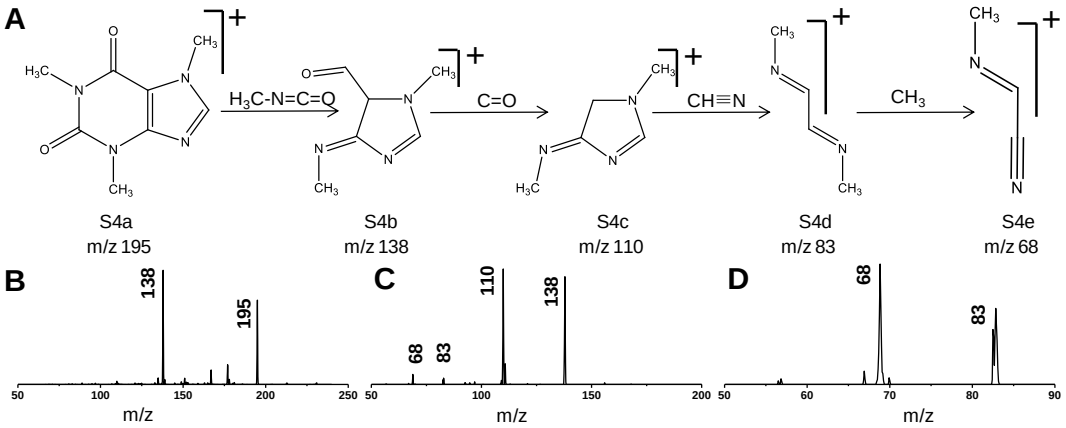

Figure S4. MS^2 and MS^3 spectra of caffeine at 2 ppt (10 pM) in solution. A) Structures of the fragments; B), C) and D) are the MS^2 and MS^3 spectra of peaks at m/z 195 and 138. Fragmentation patterns were matched with the literature.[2]

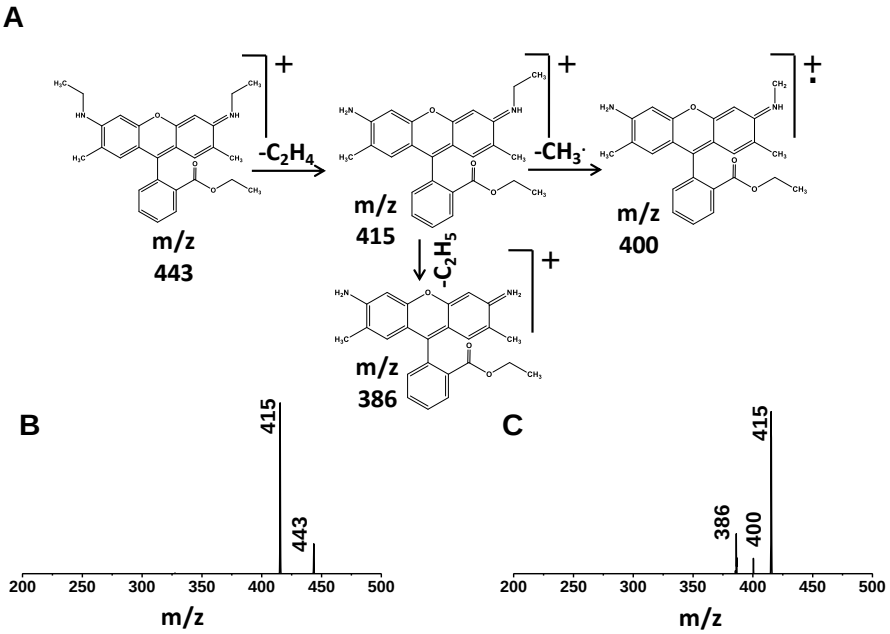

Figure S5. MS^2 and MS^3 spectra of rhodamine 6g at 4.7 ppt (10 pM) in solution. A) Structures of the fragments; B) and C) are the MS^2 and MS^3 spectra of peaks at m/z 443 and 415. The fragmentation patterns and the structures of the fragmented ions were confirmed from the literature.[3]

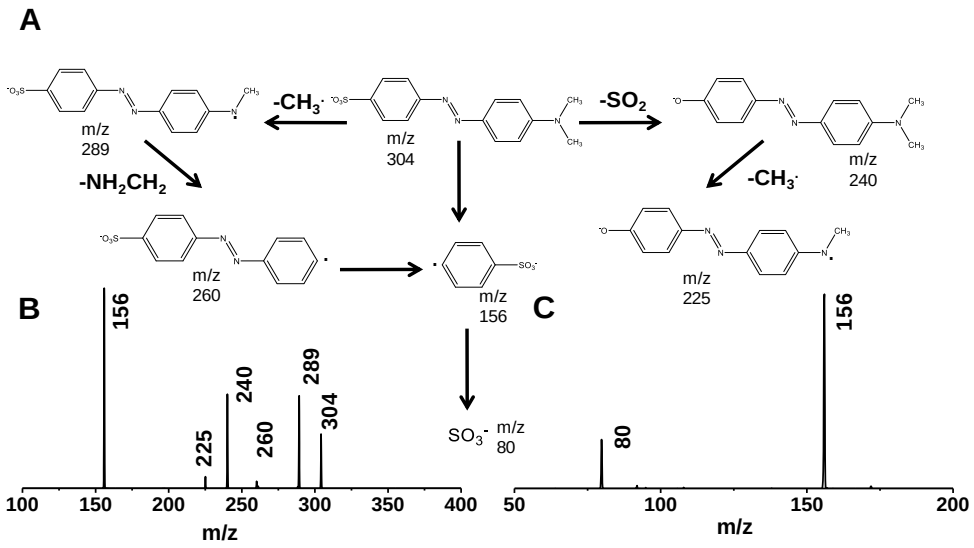

Figure S6. MS^2 and MS^3 spectra of methyl orange at 3.3 ppt (10 pM) in solution. A) Structures of the fragments; B) and C) are the MS^2 and MS^3 spectra of peaks at m/z 304 and 156. The fragmentation patterns and the structures of the fragmented ions were confirmed from the literature.[4]

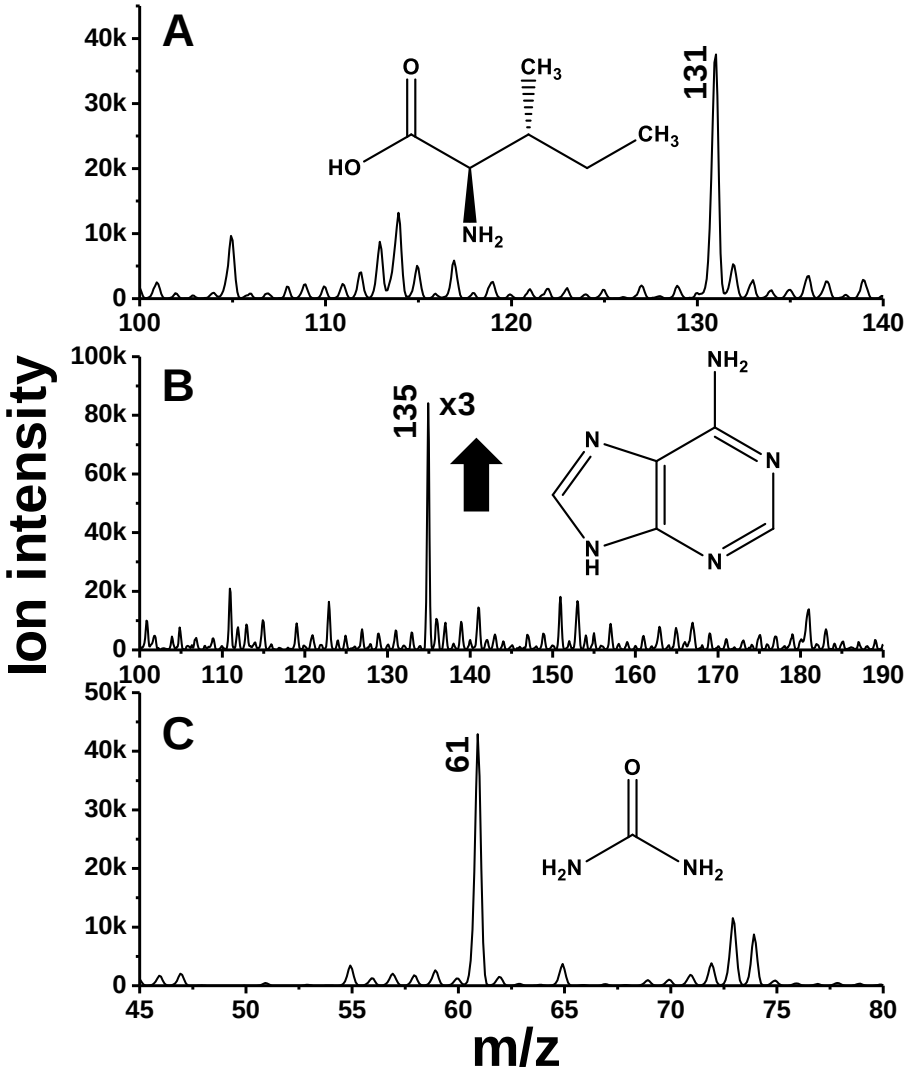

Figure S7. Mass spectra of A) isoleucine, B) adenine, and C) urea at 1.3, 1.4 and 0.6 ppt (or 10 pM) concentration.

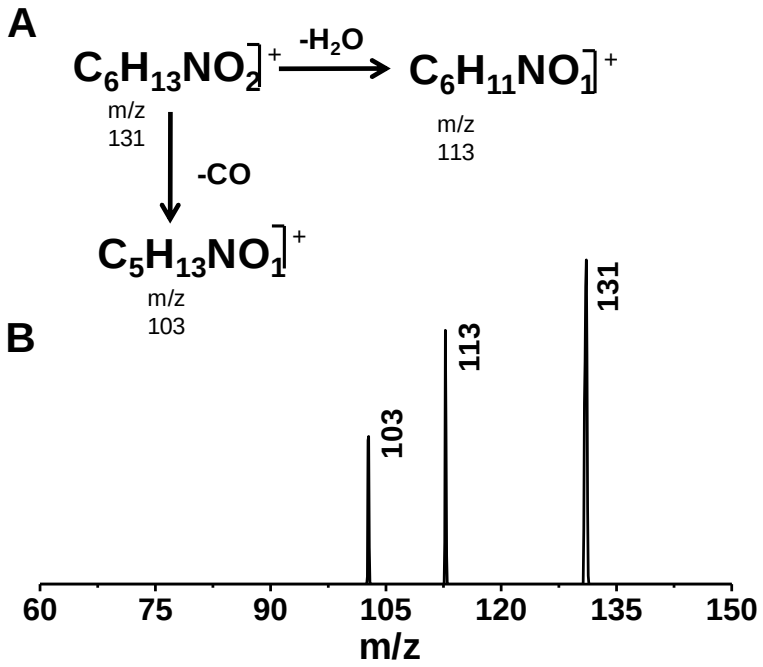

Figure S8. MS^2 spectrum of isoleucine at 1.3 ppt (10 pM) level in solution. A) Structures of the fragments and B) MS^2 spectrum of the peak at m/z 131. The fragmentation pattern and the structure of the fragmented ions were confirmed from the literature.[5]

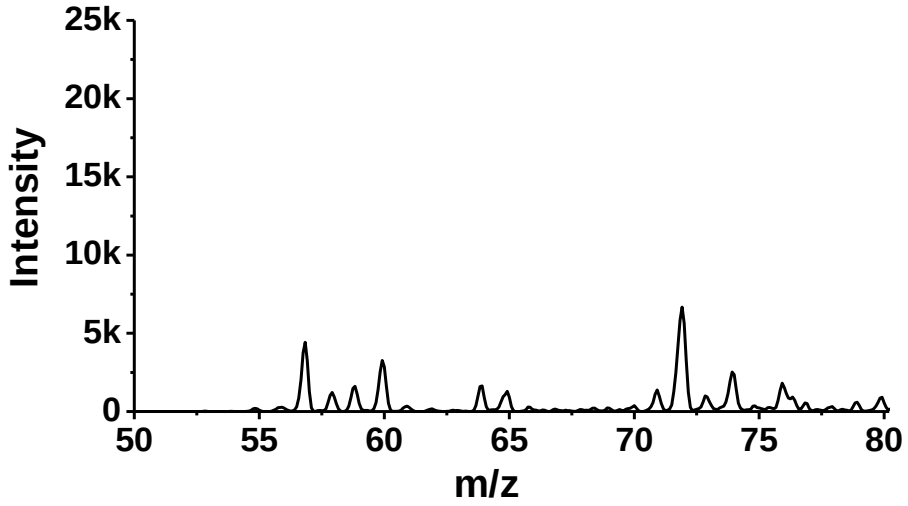

Figure S9. Blank SHPPSI mass spectrum collected by drop casting 10 µl of methanol. Mass spectrum shows absence of peak at m/z 61 in the background.

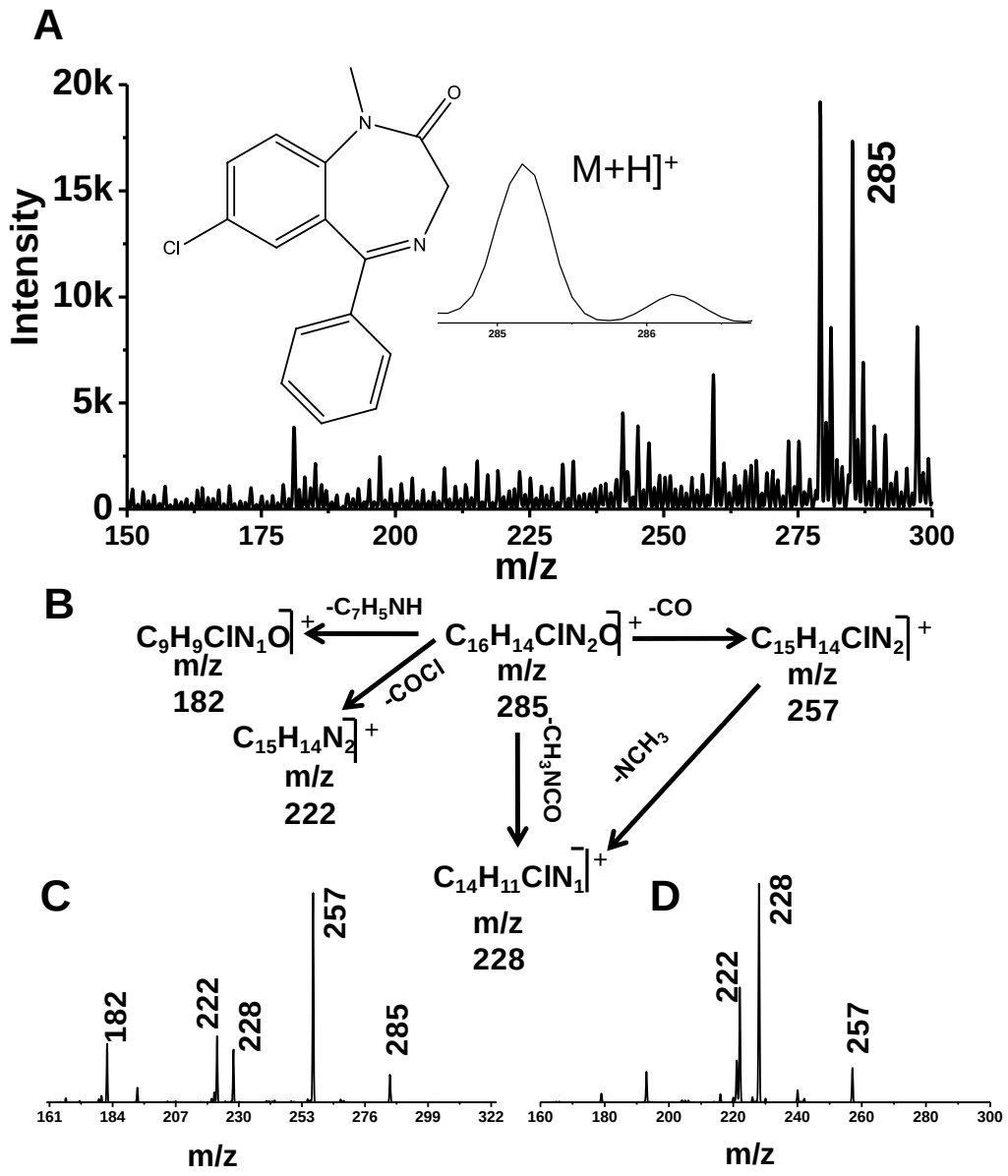

Figure S10. MS^1, MS^2 and MS^3 spectra of diazepam at 10 pM in solution. A) MS^1 spectrum of the solution; B) Structures of the fragments; C) and D) are the MS^2 and MS^3 spectra of peaks at m/z 285 and 257.[6]

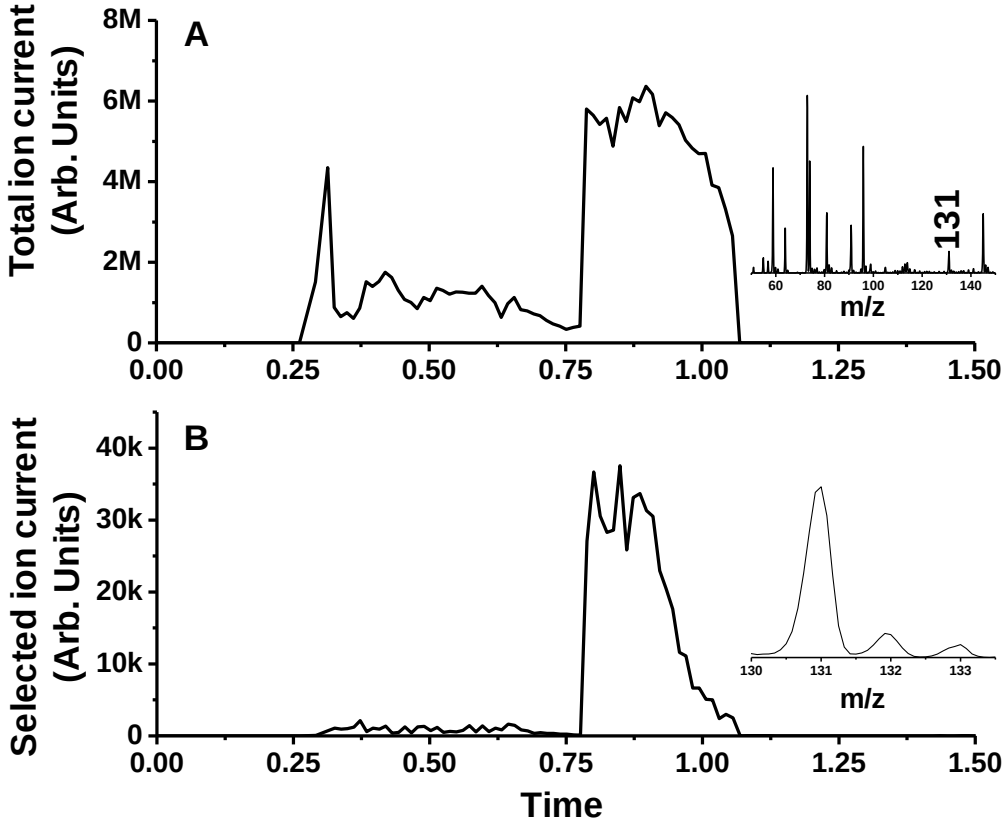

Figure S11. A) Total ion chromatogram (TIC) and B) selected ion chromatogram of (SIC) of isoleucine. Inset shows the full range mass spectrum and the spectrum in selected range.

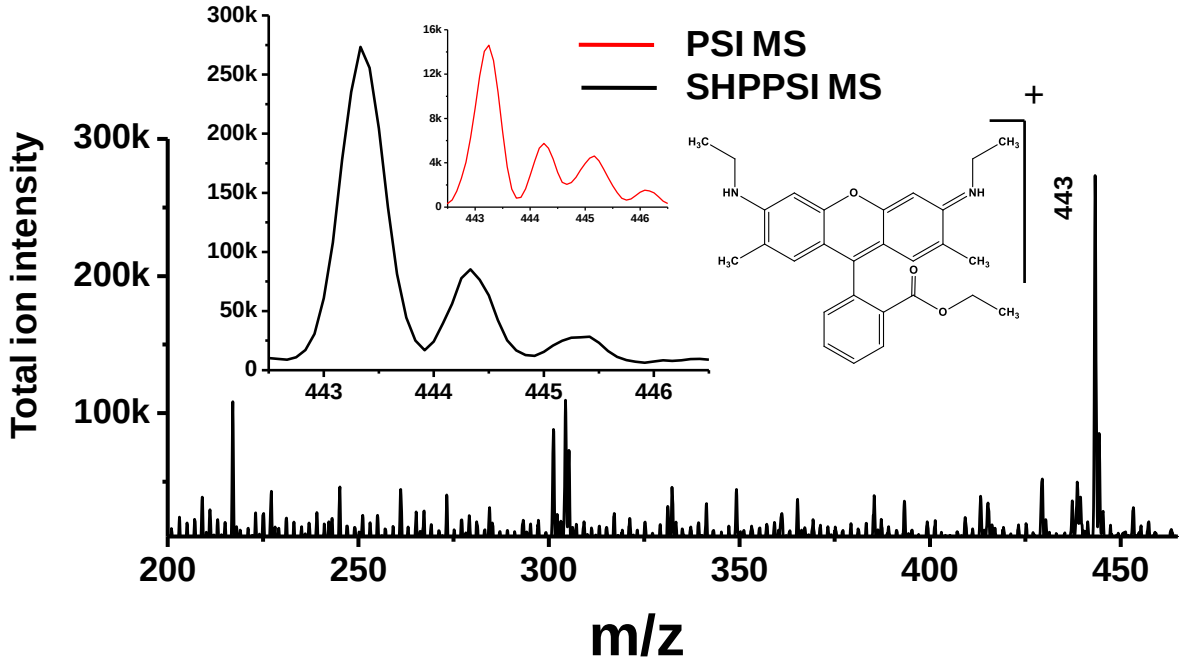

Figure S12. Full mass range mass spectrum of rhodamine 6G upon drop casting twice. The intensity corresponds to the peak 443 is almost half of the peak intensity shown in Figure 4B. It indicates that the peak intensity can be further enhanced by putting more analytes in a restricted area. Inset shows the selected area mass spectrum of the peak at m/z 443 by SHPPSI (black trace) and PSI (red trace). The intensity corresponds to two times and three times drop casting (Figure 5) in normal paper are similar due to diffusion.

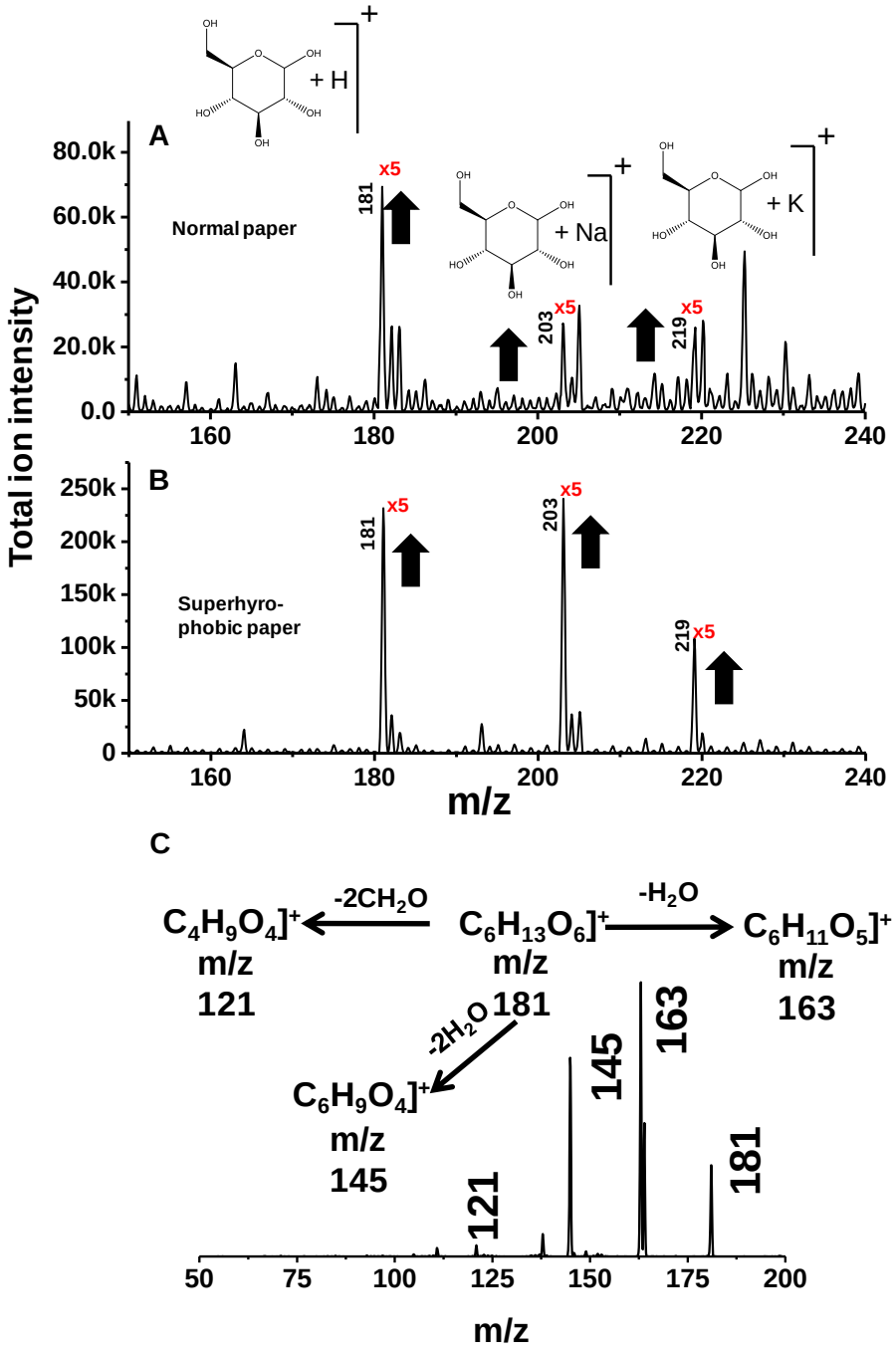

Figure S13. Comparative mass spectra of glucose in A) normal paper and B) superhydrophobic paper. C) MS^2 spectrum and the fragmentation pattern of the peak at m/z 181.[7] The intensity of the mass peaks corresponding to proton , sodium and potassium added glucose are much lower in case of normal paper than that of superhydrophobic paper. To emphasize the peak positions, the peaks have been multiplied with a factor of 5 which are indicated by upward arrows. The glucose concentration used here was 2 ppt (10 pM).

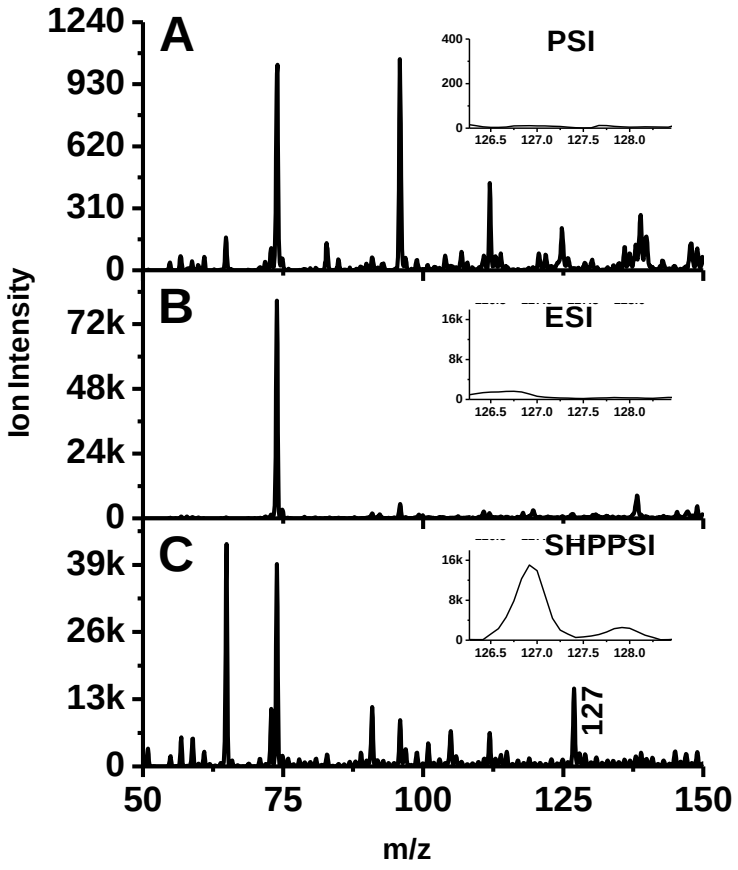

Figure S14. A) PSI, B) ESI, and C) SHPPSI mass spectra of melamine in water at 10 pM (1.2 ppt) concentration. Inset of each spectrum shows the zoomed in view of the selected peak at m/z 127, due to protonated melamine.

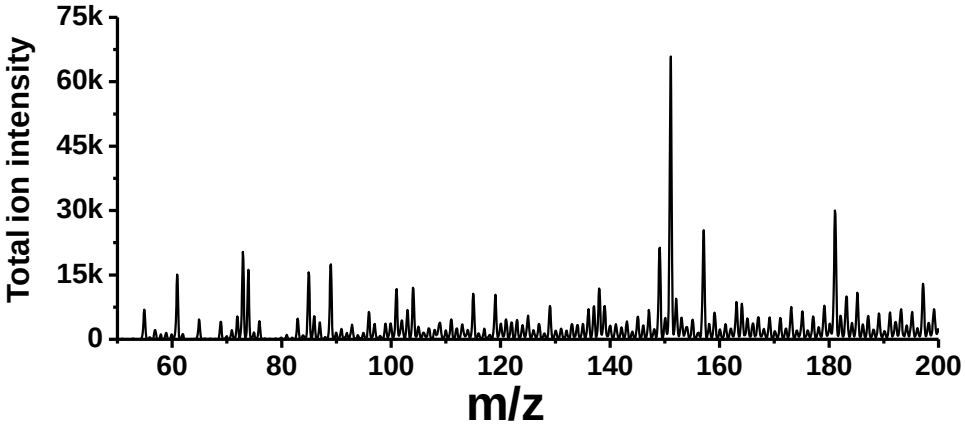

Figure S15. Mass spectrum of milk sample before spiking with melamine.

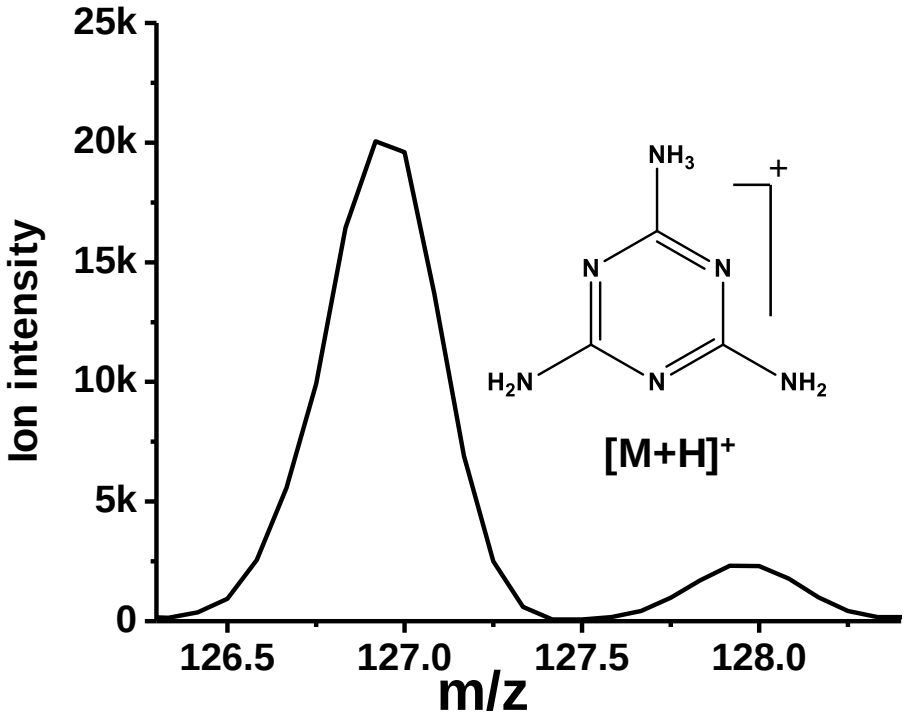

Figure S16. Mass spectrum of melamine found in laboratory-made artificially adulterated milk. Melamine concentration in the milk was 0.63 ppb (10 pM).

No.	Concentration of melamine (M)	Selected ion intensity (a.u.)	Mass spectrum
1	1.0×10^{-3}	1.66×10^{5}	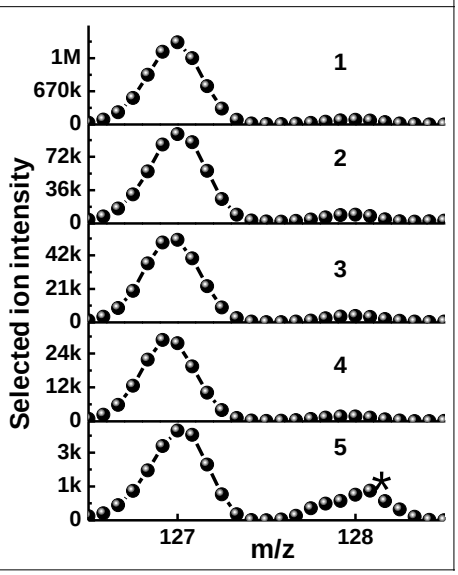
2	1.0×10^{-6}	9.65×10^{4}	
3	1.0×10^{-7}	5.17×10^{4}	
4	1.0×10^{-9}	2.76×10^{4}	
5	1.0×10^{-11}	3.44×10^{3}	

Figure S17. Mass spectra of 5 different concentrations of melamine, ranging from millimolar to picomolar. Peak labelled '*' is larger at a reduced concentration. May be it has an impurity in addition to the ^{13}C isotopic peak of melamine. The chart represents the concentration of each solution and the peak intensity of melamine at the corresponding concentration.

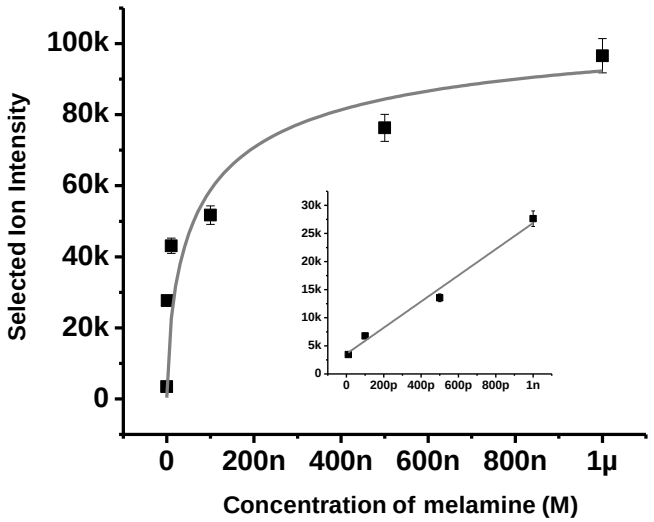

Figure S18. Calibration curve of melamine in water. Inset shows the graph at low concentrations of melamine.

References

1. Kokotou, M. G.; Thomaidis, N. S., Behavior and retention models of melamine and its hydrolysis products. *Chromatographia* **2012,** *75* (9-10), 457-467.
2. Bianco, G.; Abate, S.; Labella, C.; Cataldi, T. R. I., Identification and fragmentation pathways of caffeine metabolites in urine samples via liquid chromatography with positive electrospray ionization coupled to a hybrid quadrupole linear ion trap (LTQ) and Fourier transform ion cyclotron resonance mass spectrometry and tandem mass spectrometry. *Rapid Commun Mass Spectrom* **2009,** *23* (7), 1065-74.
3. Ferreira, B. R. V.; Correa, D. N.; Eberlin, M. N.; Vendramini, P. H., Fragmentation reactions of rhodamine B and 6G as revealed by high accuracy orbitrap tandem mass spectrometry. *J. Braz. Chem. Soc.* **2017,** *28* (1), 136-142.
4. Baiocchi, C.; Brussino, M. C.; Pramauro, E.; Prevot, A. B.; Palmisano, L.; Marcì, G., Characterization of methyl orange and its photocatalytic degradation products by HPLC/UV–VIS diode array and atmospheric pressure ionization quadrupole ion trap mass spectrometry. *International Journal of Mass Spectrometry* **2002,** *214* (2), 247-256.
5. Choi, S.-S.; Song, M. J.; Kim, O.-B.; Kim, Y., Fragmentation patterns of protonated amino acids formed by atmospheric pressure chemical ionization. *Rapid Commun. Mass Spectrom.* **2013,** *27* (1), 143-151.
6. Soparawalla, S.; Salazar, G. A.; Sokol, E.; Perry, R. H.; Cooks, R. G., Trace detection of non-uniformly distributed analytes on surfaces using mass transfer and large-area desorption electrospray ionization (DESI) mass spectrometry. *Analyst* **2010,** *135* (8), 1953-1960.
7. Taylor, V. F.; March, R. E.; Longerich, H. P.; Stadey, C. J., A mass spectrometric study of glucose, sucrose, and fructose using an inductively coupled plasma and electrospray ionization. *International Journal of Mass Spectrometry* **2005,** *243* (1), 71-84.